Delft University of Technology

Semi-Analytical Composite Oval Fuselage Weight Estimation

Roelofs, Martijn; Vos, Roelof

Semi-Analytical Composite Oval Fuselage Mass Estimation

Martijn Roelofs[*] and Roelof Vos[†]

Delft University of Technology, Delft, Zuid-Holland, 2600AA, The Netherlands

A semi-analytical mass estimation method is proposed for composite, oval fuselages, but is also applicable to conventional fuselages and to metallic materials. Loads applied to the fuselage include pressurization, steady-state maneuver loads and inertial loads. The primary structure around the passenger cabin is sized, based on first-ply failure using the Tsai-Wu failure criterion, global and local buckling. Moreover, maximum deflection due to transverse pressure is constrained for skin panels and sandwich panels. Sandwich panels are also sized for crippling and wrinkling. Empirical factors are used to calculate secondary structure and non-structural mass. In order to reduce in-the-loop calculation time, surrogate models of the sizing procedures are used, by means of neural networks. Validation of the failure calculations was done by finite-element analysis. It was found that the proposed method is capable of predicting metal, conventional fuselage mass satisfactorily, with acceptable breakdown of weights and estimated thicknesses. Additionally, the method can be used for unconventional aircraft configurations and composite material. Using composite material, a weight saving of around 19% is observed for a single-aisle aircraft as compared to aluminum.

Nomenclature

A, B, D	Extensional, coupling and bending stiffness matrices (N/m, N, Nm)	c	core
a	Panel length (m)	f	face
b	Width (m)	fr	frame
E	Young's modulus (N/m^2)	s	symmetric
G	Shear modulus (N/m^2)	si	side wall
L	Stringer length (m)	sk	skin
M	Mass (kg)	st	stringer
N	Line load (N/m)	t	Tension
p	Pressure (N/m^2)		
R	Scaling factor (-)	*Acronyms*	
S	Shear strength (N/m^2)	ACT	Advanced Composite Technology
t	Thickness (m)	ALGO	Additive Lay-up Generation Optimizer
X	Longitudinal strength (N/m^2)	ATCAS	Adv. Technology Composite Aircraft Struct.
Y	Transverse strength (N/m^2)	CLT	Classical Lamination Theory
		DOE	Design of Experiments
Greek symbols		ELFO	Enumerative Lay-up Family Optimizer
ν	Poisson ratio (-)	FEA	Finite Element Analysis
ρ	Density (kg/m^3)	GA	Genetic Algorithm
		LHS	Latin Hypercube Sampling
Subscripts and superscripts		MLG	Main Landing Gear
c	compression	MTOM	Maximum Take-Off Mass
		NEF	No Edge Free

[*]MSc Student, Faculty of Aerospace Engineering, Delft University of Technology, Kluyverweg 1 2629HS, Delft, The Netherlands

[†]Assistant Professor, Faculty of Aerospace Engineering, Delft University of Technology, Kluyverweg 1 2629HS, Delft, The Netherlands, Senior Member AIAA

American Institute of Aeronautics and Astronautics

NLG	Nose Landing Gear		Ini	Initiator
OEF	One Edge Free		fus	fuselage
Abreviations			Tor	Torenbeek
Act	Actual			

I. Introduction

The Blended Wing Body (BWB), aims to reduce fuel consumption and improve aerodynamic performance.[1] The concept is one of many novel aircraft configurations devised to compete with and replace the current conventional tube-and-wing configuration. Decades of improving this concept have exhausted the possibilities for further major improvements and thus the aircraft industry is looking for new options.

One of the challenges in designing a BWB aircraft is the fuselage, which becomes very wide and often has an airfoil-like shape in the symmetry-plane cross-section. The fuselage has to resist internal pressurization loads. It has been long-known that spheres minimize the pressure-induced stresses and are therefore the lightest structural solution. Cylinders, as used in conventional aircraft, are the most structurally efficient pressure vessels if the length needs to be larger than the diameter. This is due to the fact that the skin acts as a membrane that solely carries tension stresses. A noncircular shape develops, in addition to the tensile internal loads, internal bending moments due to the pressurization and therefore needs more material to resist these loads. Provided that the same material is used, such a pressure vessel is heavier.

Several solutions have been proposed to deal with the problem of a non-cylindrical pressurized fuselage. Most commonly, the multi-bubble concept[2] (see Figure 1(a)) and stiffened-shell concept[3] (see Figure 1(b)) are proposed. However, another concept was proposed by Vos et al.:[4] the oval fuselage. This concept, unlike the others, does not rely on members that have to be placed in the cabin to carry the out-of-plane loads and thus results in an unobstructed cabin space. The idea of this concept is that a cross-section is composed of four circular arcs, which are tangent at the connections. To carry the difference in membrane forces in these arcs, a trapezoidal structure connects the four intersections, as can be seen in Figure 1(c). The cabin is defined by a trapezoidal structure of straight panels, which intersect with the arc joints. As such, the outer skin carries the pressurization loads in pure tension. The near-vertical members panels are loaded in pure tension, while the horizontal panels (that double as floor and ceiling) are loaded in compression.
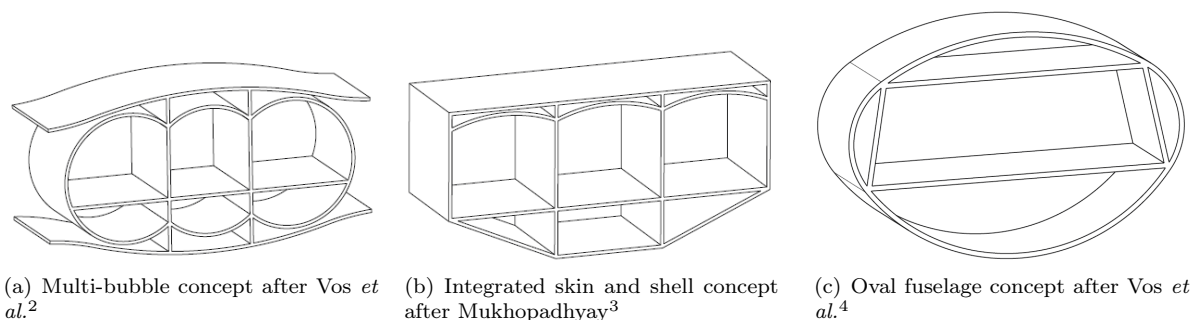

(a) Multi-bubble concept after Vos *et al.*[2]

(b) Integrated skin and shell concept after Mukhopadhyay[3]

(c) Oval fuselage concept after Vos *et al.*[4]

Figure 1. Three concepts for non-circular, pressurized fuselages produced by Schmidt and Vos[5]

Hoogreef and Vos[6] developed a fuselage parametrization method for an oval fuselage with a tapered floor and symmetrical airfoil center section as part of a BWB. In addition, a weight estimation methodology was developed that sizes the structural members based on pressurization loads, longitudinal bending and shear, and lateral loads introduced by the outer wing of a BWB (see Figure 2). The resultant hoop and the longitudinal stresses are estimated using analytical equations, assuming an nonstiffened panel. Frame weight is taken into account by applying a correction factor to the shell thickness. To predict the total fuselage weight, this method is augmented with (modified) empirical component weight estimations from Howe[7] and Torenbeek.[8] This method was further elaborated by Schmidt and Vos,[5] where the parameterization was extended to allow for a non-symmetrical airfoil shape along the fuselage centerline. The outer shell was modeled as a stiffened skin, while the trapezoidal structure consisted of sandwich panels. Plane stress assumption were used and all structural members were sized based on a set of ten load conditions. Dimpling, crimping, wrinkling and global buckling of these sandwich beams were taken into account. Inertial and

American Institute of Aeronautics and Astronautics

aerodynamic loads are obtained at each cross-section by representing the fuselage as a 1-dimensional beam. Furthermore, frames were sized based on shell-buckling criteria of circular tubes. It was shown that the resulting weight estimation correlated better to weight data from the open literature than various handbook methods, although for some aircraft the method still had an error of 20%. In order to validate the stress analysis method, a finite element analysis (FEA) was carried out by De Smedt and Vos.[9] It was shown that there was good correspondence in lateral direct stress and hoop stresses, while longitudinal direct stresses and longitudinal shear stresses showed significant differences.

To improve the weight estimation methodology, this paper discusses an alternative approach to the structural analysis of the oval fuselage based on the idealized-structure assumptions. In addition, the presented method is also extended towards the use of composite materials. The present method is implemented in a conceptual aircraft synthesis tool called the *Initiator*.[10] The Initiator is used to size and analyze conventional and unconventional aircraft based on a user-specified set of top-level requirements. The process flow of a design convergence loop is shown in Figure 3, where it can be seen that the Initiator's design process can be divided into three major blocks: Class I, Class II and Class II.5. The present fuselage weight estimation method fits in the Class II.5 block of the Initiator. The convergence process of the Initiator is iterative implying that the weight estimation method of the

Figure 2. Notional cross section of oval fuselage with applied forces.

fuselage is dependent on the characteristic masses of the aircraft (i.e. maximum take-off mass, maximum zero-fuel mass, and design landing mass) but is also part of these masses. The weight estimation method converges based on predefined thresholds for the change in maximum take-off mass, aerodynamic efficiency, and fuel mass between two subsequent iterations.
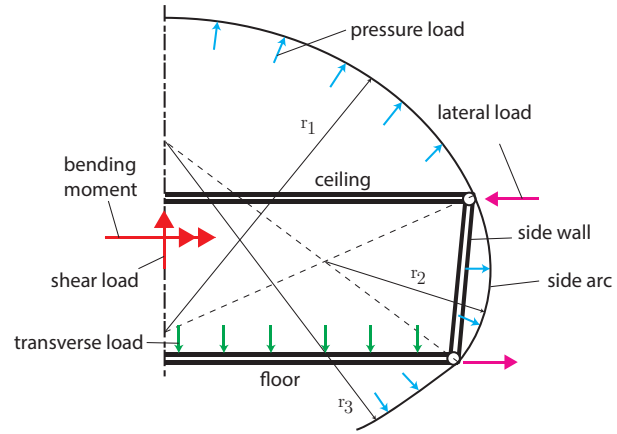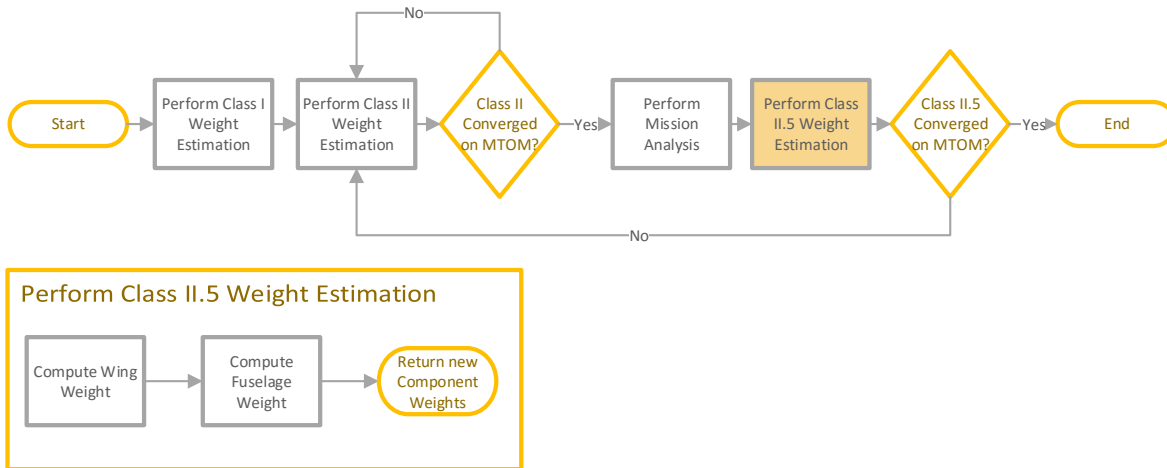

Figure 3. General Process Flow of Initiator

In the subsequent sections the structural analysis and mass estimation method is presented (Section II). The sizing of the inidividual structural components is detailed in Section III. The results of the analysis methodology are compared to a higher-order method in Section IV. In addition, the mass estimation is verified for the individual structural components of the fuselage. The paper closes with conclusions on the applicability and validity of the presented method and makes recommendations for further research.

American Institute of Aeronautics and Astronautics

II.   Structural Mass Estimation Methodology

In this section, an overview of the mass estimation method is presented. Figure 4 shows the flowchart of the mass estimation method, including the convergence loop. It should be noted that this method itself is part of the larger convergence loop built into the Initiator, which ensures all aircraft masses become consistent between all implemented mass estimation methods, as shown in Figure 3. The structural sizing method starts with the Class II mass estimation. It subsequently needs an initial value for all the structural design variables. If the mass estimation has been run before (i.g. for a previous load case) it will use that solution as a starting point. Otherwise, it will use a predefined initial design vector. Based on a preselected load case the aerodynamic and inertial moment and shear force distributions in longitudinal direction are computed. In addition, transverse loads on the floor of the fuselage as well as (potential) lateral loads on the internal trapezoidal structure of the fuselage are added. The latter could stem from the attachment of a wing if the oval fuselage is part of a blended-wing body (as in Schmidt and Vos[5]). Finally, loads are exerted on the outer skin panels and trapezoidal structure due to pressurization. These combined loads are exerted on an idealized structural representation of outer skin of the fuselage, where the panels only carry shear stresses and the booms only carry normal stresses. Based on predefined stress and buckling allowables, each of the booms and panels is sized until the solution converges within a predefined tolerance. The mass is subsequently obtained by multiplying the material density with the volume of the structure.

The mass estimation method makes use of a set of twelve different load cases: four load cases for a 2.5g pull up maneuver (at MTOM and at MZFM and with or without pressurization loads), four load cases for a -1.5g push-over maneuver, two load cases for a 2.5g landing at maximum landing mass, and two load cases for vertical gusts at MZFM. In all conditions, the presence of the maximum structural payload is assumed. The aerodynamic loads are computed using a vortex lattice method which model solely the wing and the horizontal tail plane. Inertial loads are introduced as point masses when the component mass is concentrated in a small volume (i.e. landing gear legs, passengers, avionics, or the engines) or distributed when the component encompasses a large volume (i.e. the wing, the fuselage or the tail surfaces). Pressurization loads are computed using a two-dimensional analysis of the oval fuselage barrels as shown in Figure 2 and detailed by Schmidt and Vos.[5]

As can be seen in Figure 5, all forces that act on the aircraft (aerodynamic, ground loads, and inertial loads) are mapped onto a one-dimensional Euler-Bernoulli beam that spans the length of the passenger cabin and excludes the tail cone and the nose cone of the fuselage. The resultant loads of the wing for each load case are introduced as a combination of a discrete force and moment at the location where the front spar intersects the fuselage symmetry plane. The same holds for the empennage structure
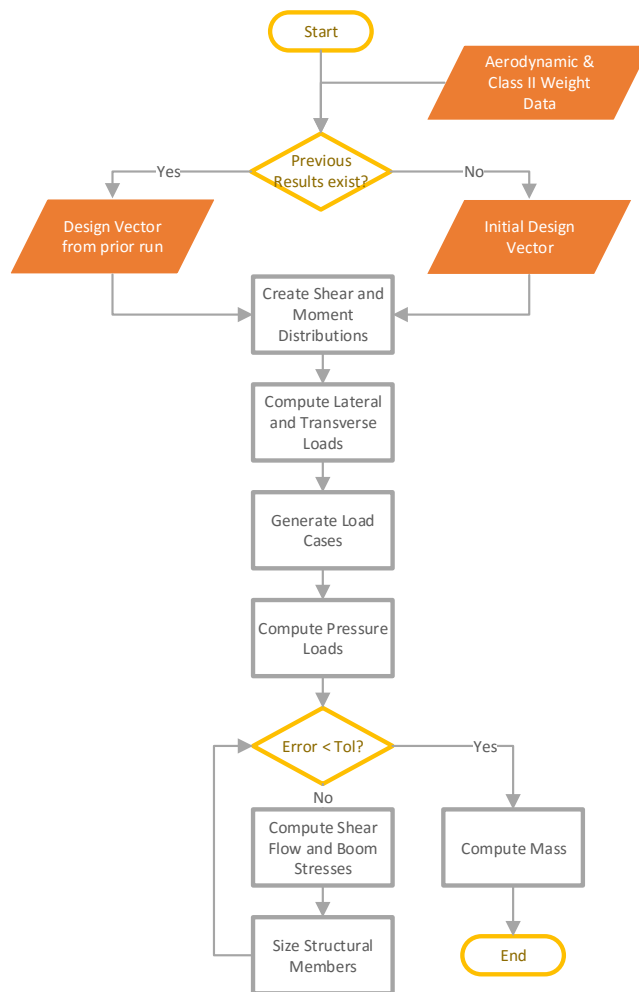

Figure 4. Fuselage mass estimation process flow

American Institute of Aeronautics and Astronautics

that includes the horizontal tail plane. The ground loads are introduced through the nose landing gear (NLG) and main landing gear (MLG) at their respective locations. The combined forces and moments result in a shear force and bending moment distribution.
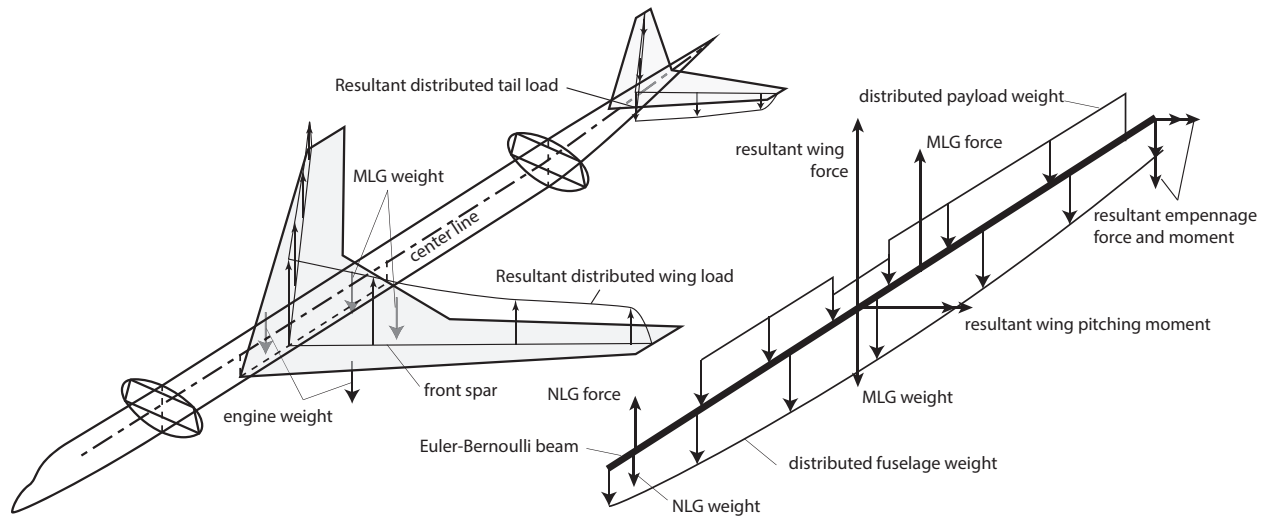

Figure 5. Distributed and discrete forces and moments of wing and tail (left) are mapped onto a one-dimensional Euler-Bernoulli beam (right). The resultant distributed wing load includes the wing weight, the fuel weight, and the aerodynamic load. The resultant distributed fuselage load includes the fuselage structural and nonstructural weights. The distributed payload consists of passengers and freight. Note that not all component weights that are included in the method are shown in this figure.

As shown in Figure 6 the structural model can be decomposed in two parts: the outer shell, which is modeled as an idealized structure, and the floor and ceiling, which are modeled as sandwich structures. The oval outer shell is analyzed as a single-cell section, with the thickness of the 'vertical' walls added to the side arc thickness. Through this assumption, the ceiling and floor members carry no shear flow, while the wall member shares the shear flow with the side arc. To compute the internal stresses in the outer shell due to the bending moment and shear force distribution, a boom method is applied. Following Megson,[11] the boom method is adapted to account for tapering of the fuselage. The fuselage is divided in N longitudinal sections and K circumferential stations. The longitudinal booms represent the stringers in between the sections, while the circumferential booms represent the frame sections. The booms carry the direct stresses that result from the bending moment and shear force distribution. The skin panels between the booms carry the shear stresses that result from the shear force distribution. In addition, these outer-shell skin panels also carry the pressurization three different pressurization loads: longitudinal stresses, hoop stresses and transverse (through-the-thickness) pressure loads.

The resultant forces at the junctions of the circular arcs (i.e. due to pressurization) are exerted on the floor, ceiling and side-wall structures. Since the floor and ceiling are loaded in compression due the pressurization loads, they are modeled as a sandwich structure that each consists of a core and two symmetric facing sheets. The floor structure is also subjected to a transverse load that results from the payload weight. The side walls are assumed to take up the tensile loads that result from pressurization. They are modeled as a monolithic side panel. All members of the trapezoidal box structure are assumed to be simply supported at the junction points.

The mass of the fuselage consists of the mass of the primary structure, the mass of secondary structure and nonstructural components. If a metal fuselage is assumed, the structural mass estimations for the fuselage nose cone, tail cone, crew floor, windscreen, front pressure bulkhead, rear pressure bulkhead, and cargo floor of Howe[7] are used as described in Vos and Hoogreef.[6] If a composite structure is assumed, trends from NASA's Advanced Composite Tecnology (ACT) program and Boeing's Advanced Technology Composite Aircraft Structure (ACTAS) are used.[12,13] The combined structural mass for window belts, door reinforcements and splicing assembly are estimated to weigh 17% of the side quadrant primary structure mass (frames, stringers and outer skin). The cargo floor mass is estimated to weigh 26% of the primary structure of the keel quadrant, while the splicing assembly amounts to 11% of the keel quadrant. The mass of the fuselage nose and tail cone are estimated by taking the average total smeared thickness in the side

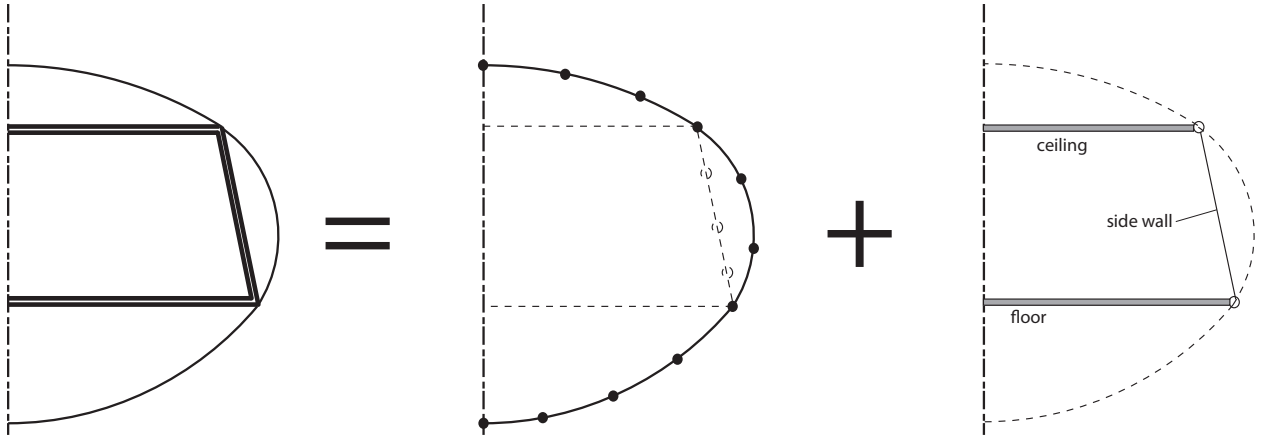American Institute of Aeronautics and Astronautics

Figure 6. Notional overview of how the oval fuselage cross-sectional structure is modeled. An idealized structure is assumed for the circular fuselage panels where the side wall is unified with the side arc. The floor and ceiling are modeled as sandwich structures while the side wall is modeled as a monolithic plate.

panels and multiplying this by the surface area of these two components.

The mass of the fuselage barrel between nose cone and tail cone and without cut-outs or assembly splices (M_{barrel}) is computed by summing the mass of all skin panels (sk), stringers (st), frames (fr), sandwich panels and side walls (si):

$$M_{\text{barrel}} = \sum_{n=1}^{N-1} l_n \Big[\sum_{k=1}^{K} \big(\rho_{\text{st}} A_{\text{st}_{n,k}} + \rho_{\text{sk}} s_{n,k} t_{\text{sk}_{n,k}} \big) +$$

$$\sum_{j=1}^{2} w_n \big(\rho_{\text{c}} t_{\text{c}_n} + 2\rho_{\text{f}} t_{\text{f}_n} \big) + 2\rho_{\text{si}} h_n t_{\text{si}_n} \Big] + \sum_{n=1}^{N} \sum_{k=1}^{K} \rho_{\text{fr}} s_{n,k} A_{\text{fr}_{n,k}} \tag{1}$$

where $l_{n,k}$ represents the length in longitudinal direction between section n and section $n+1$, $s_{n,k}$ is the arc length between circumferential station k and station $k+1$ at longitudinal section n, w_n is the width of a floor or ceiling structure at section n, h_n is the length of a side wall at section n, A is the cross sectional area, and t is the thickness. The density (ρ) for each of the components is input to the method as are the number and location of longitudinal and circumferential sections. The thicknesses of skin, side wall, core (c) and face sheets (f), as well as the cross-sectional area of frames and stringers are found from the sizing process that is further detailed in Section III.

While frame and and side wall sizing is computationally inexpensive, the sizing methods for (sandwich) panels and stringers outlined requires too much in-the-loop computation time for use in the Initiator. Therefore, surrogate models in the form of neural networks are employed to relate the output data (e.g. panel thickness, stringer cross-sectional area) to the input (i.e. panel dimensions (a, b) and applied loads, N_x, N_y, $N_x y$). The bounds on the inputs for this method are shown in Table 1 for monolitichic panels, stringers, and sandwich panels, respectively. Latin Hypercube Sampling (LHS) is used to perform a design of experiments (DOE) and sample the design space between these bounds. The results are subsequently used to train the neural networks.

III.   Composite Member Sizing

As was shown in Figure 4, each iteration of the mass estimation method, the boom method and sizing procedures of the primary structure are performed. Together, these determine the thicknesses or cross-sectional area of the structural members and therefore the fuselage mass. This section elaborates on the methods used to analyze failure of skin panels, sandwich panels, stringers, and frames. Additionally, a deterministic optimization approach is discussed for each of these three components, which aims to find the most suitable laminate stacking sequence and dimensions of each component, based on the applied loads.

American Institute of Aeronautics and Astronautics

Table 1. Range of input values that are sampled by the DOE for monolithic panels (left), stringers (center) and sandwich panels (right).

Monolithic panel				Stringer				Sandwich panel		
Input	Start	End		Input	Start	End		Input	Start	End
a [m]	0.25	0.8		L [m]	0.3	0.6		a [m]	0.1	5.0
b [m]	0.1	0.5		$N_{x,\text{comp}}$ [kN]	0	2000		b [m]	0.1	0.8
N_{xy} [kN/m]	0	800		$N_{x,\text{tens}}$ [kN]	0	2000		N_x [kN/m]	0	500
p [kPa]	0	100						N_y [kN/m]	0	500
N_y [kN/m]	0	500						N_{xy} [kN/m]	0	800
N_x [kN/m]	$= N_y/2$							p [kPa]	0	100

A. Monolithic Plate Sizing

Optimization of monolithic plates is performed according to the Additive Lay-up Generation Optimizer (ALGO) routine developed by Van Gent and Kassapoglou.[14] However, the pressurization loads are added to the process. Figure 7 shows the optimization process.

As a start, a $[\pm 45/0/90]_\text{s}$ laminate is used. Then this laminate is analyzed, which means all failure modes are checked. If no failure is found, the laminate is valid and the optimization ends. If not, a ply is added such that the most critical load is reduced. Additionally, in the second and later iterations, four alternatives for the main laminate are created which may satisfy the failure criteria by having slightly more thickness. All five (including the main laminate) designs are analyzed and the main laminate is replaced with the thinnest option capable of withstanding the loads. If no designs can handle the loads, the main laminate is modified again. When the plate is found to be shear buckling critical, it is not directly evident what ply should be added. Therefore, each D-term is perturbed by 1% and the shear buckling calculation is performed for each perturbation separately. The term that gives the largest increase in critical shear buckling load determines the ply that should be added in the next iteration.

Finally, when a suitable laminate has been found, an iterative technique starts that tries to remove as many plies from the laminate without making it fail. Since the optimization may jump from one critical failure mode to another, some redundancy may develop in the laminate. This process aims to minimize the weight penalty associated with that.

The stresses in the members and laminate properties are computed using Classical Lamination Theory (CLT) according to Jones.[15] Failure is checked with first-ply failure using the Tsai-Wu criterion. All strengths are decreased by three knockdown factors: elevated temperature wet, barely visible impact damage and material scatter.[16] The values for these knockdown factors are 0.8, 0.65 and 0.8, respectively. An approximate method to obtain the critical shear buckling load is presented in Kassapoglou[16] and used in the present work. For panels with an aspect ratio between 0.5 and 1 an empirical relation is used, while for aspect ratios below 0.5 a different, semi-analytical method is used. As an additional failure mode, a maximum deflection of the skin panel is imposed when under pressure loading. Again, the methodology from Kassapoglou[16] is employed.

B. Sandwich Panel Sizing

Sandwich panels are assumed to be used for the trapezoidal structure. They are loaded in compression and by a transverse load due to passenger weight. A sandwich panel consists of two facesheets and a core of, for example, honeycomb material. The ABD matrices of the facesheets can be determined using CLT, since these are just normal laminates. However, the sandwich in its entirety has a different D matrix, for which the failure modes of a sandwich panel can be computed. First of all, there is global buckling under compression. Secondly, shear buckling and buckling under the combined load case (compression and shear). Thirdly, sandwich wrinkling (symmetric ans asymmetric) under compression and shear is taken into account. To obtain conservative estimates for this failure mode, waviness is taken into account. Sandwich crimping is the final failure mode.

For the sandwich panels, the same analysis is used as for monolithic panels under transverse pressure. The optimization process for sandwich panels is identical to the ALGO routine as presented for panels in Figure 7.
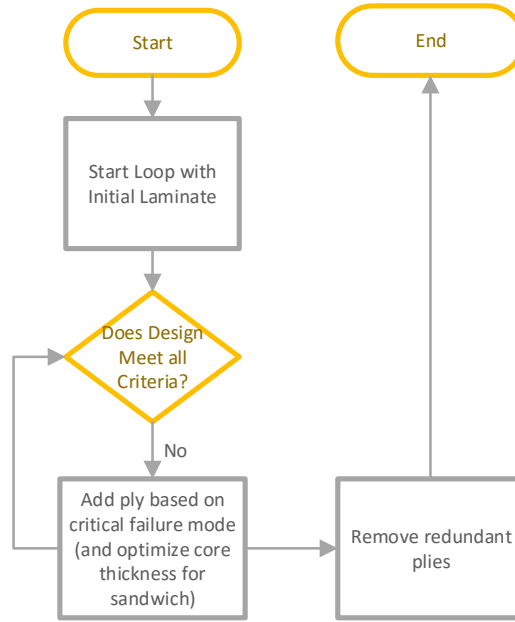
American Institute of Aeronautics and Astronautics

Figure 7. Optimization Process for Composite (Sandwich) Panels

In addition to the analysis of additional failure modes of sandwich panels, a core thickness optimization loop is performed each time the face laminate is analyzed. This loop increases the core thickness from a predefined minimum (0.1 mm) to a predefined maximum (200 mm), or until all failure criteria are met.

C. Stringer Sizing

The Enumerative Lay-up Family Optimizer (ELFO) by Van Gent and Kassapoglou[14] is used to optimize a stringer for a maximum tensile and maximum compression load simultaneously. ELFO aims to include as many 0 plies as possible, since only axial loads are considered for stringers. Furthermore, basic laminate design rules are used, including but not limited to: balanced and symmetric laminates, hte 10% rule and the maximum-pl-stack rule.

ELFO generates a family of laminates, which are subsequently applied to each member (flange or web) of the stringer under consideration. Each member can have a different laminate, and a maximum difference in amount of plies is set, such that excessive ply-drops from one member to another are prevented. With the laminates fixed, ELFO starts a gradient based optimization routine to determine the optimal flange widths (i.e. minimum weight, while satisfying failure constraints). When all different combinations of layups have been analyzed, the lightest design meeting the criteria is chosen, concluding the procedure. A flowchart of the described process can be seen in Figure 8.
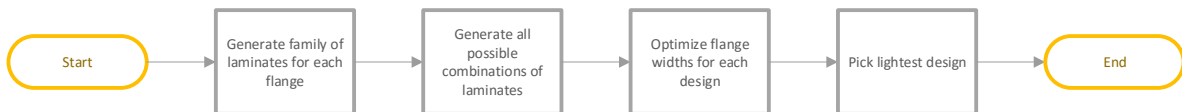

Figure 8. Optimization Process for Composite Stringers

Only C-stringers are modeled in the present study. Flanges of a stringer feature a local stability failure mode, called crippling, where the flange buckles locally under compression. A semi-empirical approach is

American Institute of Aeronautics and Astronautics

used, based on Kassapoglou.[16] The web is analyzed as a no-edge-free (NEF) member, while the top and bottom flanges are analyzed as one-edge-free (OEF) members. Finally, column buckling failure is analyzed. Pinned boundary conditions are assumed at both beam ends.

D.   Frame Sizing

The elastic center method as presented by Bruhn[17] was used for sizing of the fuselage frames. As such, the shear forces from the boom method can be taken into account to compute the internal bending moment in a frame. This moment then is used to size a cross-section that minimizes the weight while preventing material failure and crippling. Finally, a minimum cross-sectional area moment of inertia results from the Shanley criterion, in order to prevent global buckling of the fuselage structure.

IV.   Verification & Validation

A.   Pressure Load Validation

FEA of an oval section with internal pressurization was performed using Abaqus. In order to model the pressure loads, symmetry boundary conditions were applied to the front and rear edges of the section, as well as the edges in the symmetry plane. A pressure of 45 kPa was applied and the Poisson's ratio of the material was set to 0.5, modeling a perfectly incompressible material. This way no load alleviation takes place due to contraction of the section in the longitudinal direction.

The exact values from the analytical method and an average of the FEA results are shown in Table 2. It can be seen that both the hoop and longitudinal stresses are approximated accurately. On a critical note, though, the presented section is straight, i.e. the cross-section does not change in longitudinal direction. Therefore the analytical solution for pressurization stress holds. Further research has to point out whether such good agreement is maintained when the fuselage shape is more complex (i.e. changes in longitudinal direction).

Table 2. Comparison of FEA and analytical hoop pressure stress

Member	FEA [MPa]	Analytical [MPa]	Error
Arc 1	35.4	35.3	-0.28%
Arc 2	10.5	10.5	0%
Arc 3	26.8	26.7	-0.37%
Ceiling	-10.9	-11.0	-0.92%
Wall	8.00	8.05	0.63%
Floor	-7.2	-7.17	0.42%

B.   Boom Method Verification and Validation

The implementation of the boom method is verified by examining the direct stress resulting from the applied bending moment and the shear flow resulting from the applied shear forces. Because a symmetrical cross-section was assumed and all loads are applied in the axis of symmetry, it is expected that both the stress and shearflow distributions along the cross-section are symmetrical (for stress exactly equal, for shear flow equal magnitude, opposite sign). Moreover, the shear flow becomes zero at exactly the top and bottom of the cross-section and has a maximum in between. The direct stress is maximum at the top or bottom of the fuselage.

To test above statements, an arbitrary oval cross-section was created and a fuselage section of approximately 5 m was created. A constant shear force of 998.8 kN and constant bending moment of 9,537.6 kNm were applied, where the bending moment is oriented such that the upper side of the fuselage is in compression (which is not necessarily an actual load case). The resulting boom stresses and shear stress computed by the boom method are shown in Figure 9(a) and Figure 10(a), respectively.

As can be seen from Figure 9(a), the stress is indeed negative in the upper portion of the fuselage section and its positive maximum is exactly at the bottom. However, the minimum is located at the junction of the top and side arc (and ceiling and wall). The stress shown in this figure was scaled to the smeared stringer
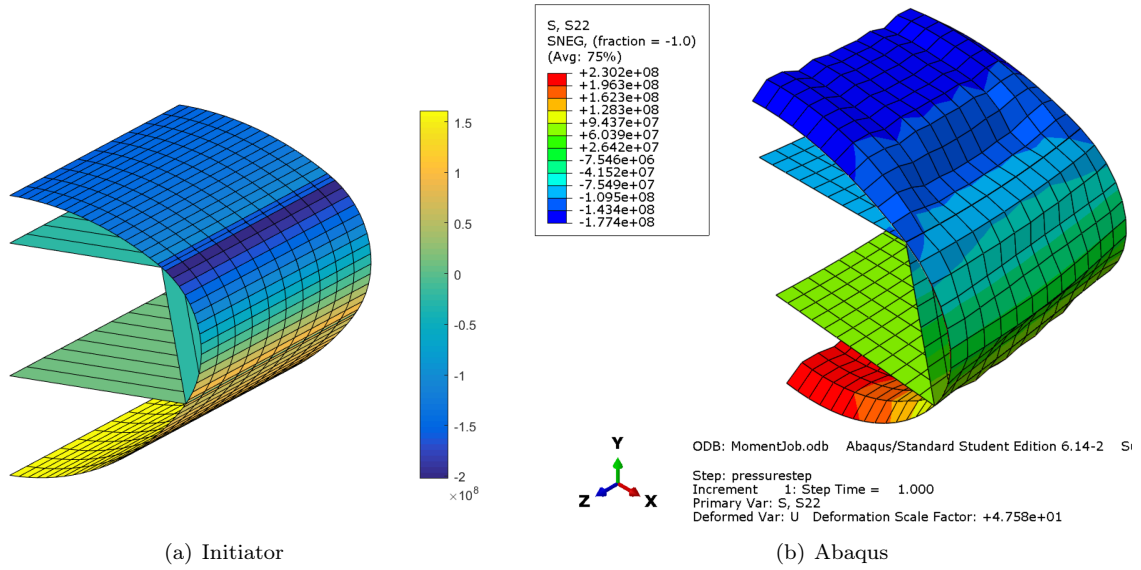
American Institute of Aeronautics and Astronautics

(a) Initiator   (b) Abaqus

Figure 9. Direct Stress

thickness (for comparison with FEA, presented hereafter), which is not equal to the boom stress. Because the boom areas include the skin and those in the side arc also the wall, the boom stress is different from the actual stress in the (smeared) stringers. This also explains the jump in direct stress observed in Figure 9(a) and why the minimum stress is not observed in the top of the section.
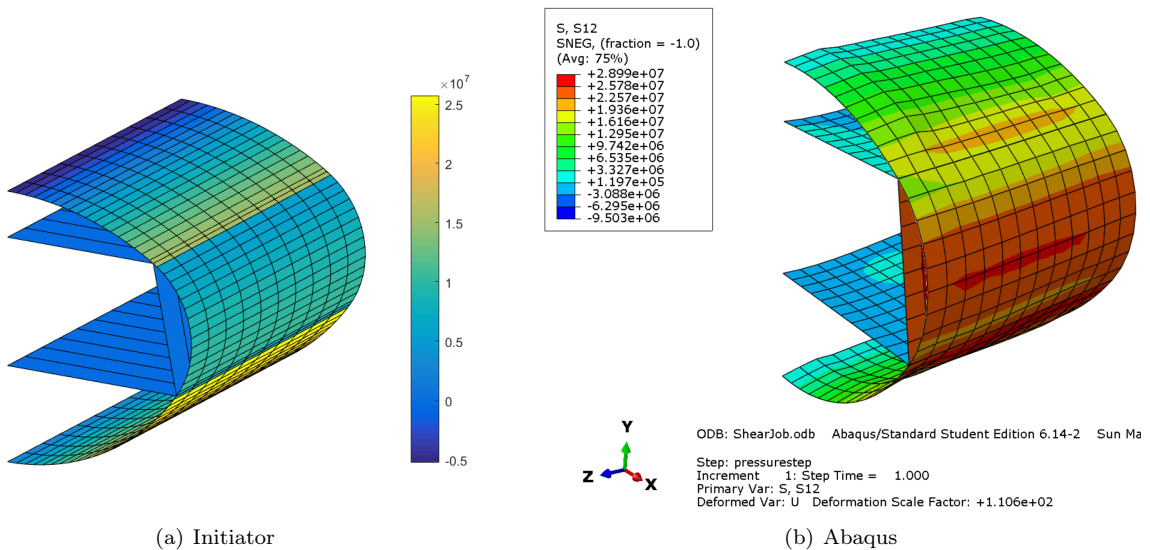

(a) Initiator   (b) Abaqus

Figure 10. Shear Stress

Figure 9(b) and Figure 10(b) show the same fuselage section as discussed earlier, but now modeled using Abaqus. No stringers were modeled; instead the smeared stringer thickness was used to model the stringers as a skin. Even with this approximation and the difference that in the FEA model a trapezoid structure is present, which is omitted in the boom method, good agreement is reached between the boom method and FEA. As expected, the signs of both direct and shear stress are identical for both methods. More interestingly, the magnitude of both stresses is also similar for both methods, giving confidence in the implemented boom method.

American Institute of Aeronautics and Astronautics

C. Panel Failure Validation

The shear buckling analysis that is implemented in the ALGO method is checked with FEA results. Three different panel dimensions, representing three different aspect ratios, are tested. For each panel, multiple shear loads are applied. First, the analytical method is run to optimize a certain laminate for that specific panel and load combination. Secondly, that panel with the optimized laminate is modeled in Abaqus and a buckling analysis is performed to see whether the failure modes match. The boundary conditions in Abaqus resemble a simply supported plate, which is also assumed in the analytical methods. The material used in the present study is defined in Table 3 and is taken from Kassapoglou.[16]

Table 3. Material properties

Unidirectional material		
Property	Value	Unit
E_x	137.9	GPa
E_y	11.7	GPa
ν_{xy}	0.29	-
G_{xy}	4.82	GPa
t_{ply}	0.1524	mm
X^t	2068	MPa
X^c	1723	MPa
Y^t	96.5	MPa
Y^c	338	MPa
S	124	MPa
ρ	1609	kg/m^3

Core material		
Property	Value	Unit
E_c	131	MPa
G_{xz}	41.4	MPa
G_{yz}	20.7	MPa
ρ	48.2	kg/m^3

The results of the analytic shear buckling analysis and the FEA are shown in Figure 11. In Figure 11(b) and Figure 11(c) it can be seen that fairly good agreement is achieved between the analytical method and the FEA. The error ranges from 5% to 20% and from 13% to 66%, respectively. The square panel shear buckling failure as obtained from Figure 11(a) shows a large error which is approximately constant around 55 %. Note that the analytical results in Figure 11(a) and Figure 11(b) are obtained using an empirical relation, while Figure 11(c) is computed using a semi-analytical relation, as was mentioned in Section III-III-A.

(a) Panel shear buckling failure for $a/b = 1$

(b) Panel shear buckling failure for $a/b = 0.75$

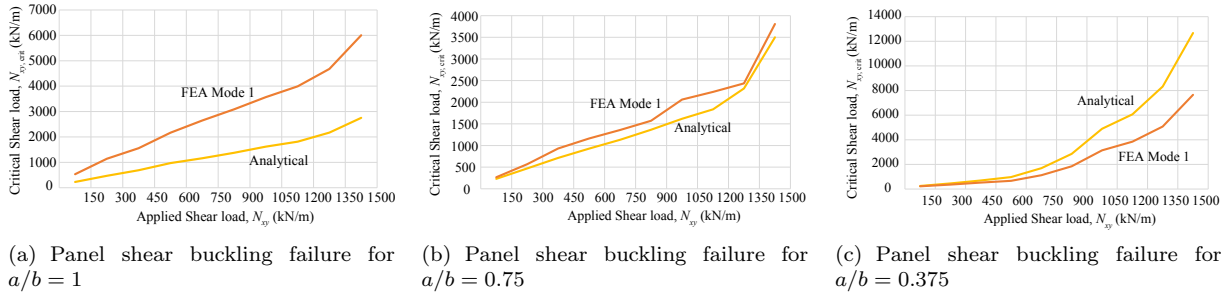(c) Panel shear buckling failure for $a/b = 0.375$

Figure 11. Validation results for panel shear buckling

The difference in Figure 11(a) is large, but a conservative result is obtained since a lower critical load is predicted by the analytical approach. Additionally, panels of this aspect ratio are rarely found in fuselage structures. However, the results from Figure 11(c) are applicable to panels in fuselage structures and these results are non-conservative. In order to account for this, the estimated critical shear buckling load may be scaled to more closely represent the FEA data. A scaling factor obtained from Figure 11(c) is provided by:

$$R_{N_{xy}} = 0.88846 \cdot N_{xy}^{-0.16974} \tag{2}$$

This factor should be multiplied by the analytical result to obtain the FEA result. Note that the unit for N_{xy} is kN/m.

American Institute of Aeronautics and Astronautics

Additionally, the maximum deflection of panels under transverse pressure is compared with FEA predictions. A pressure of 60 kPa was applied to panels with a length of 0.8 m and varying widths. The results are shown in Figure 12, where good agreement is observed between the analytical result and the FEA result. The maximum error is around 4%.
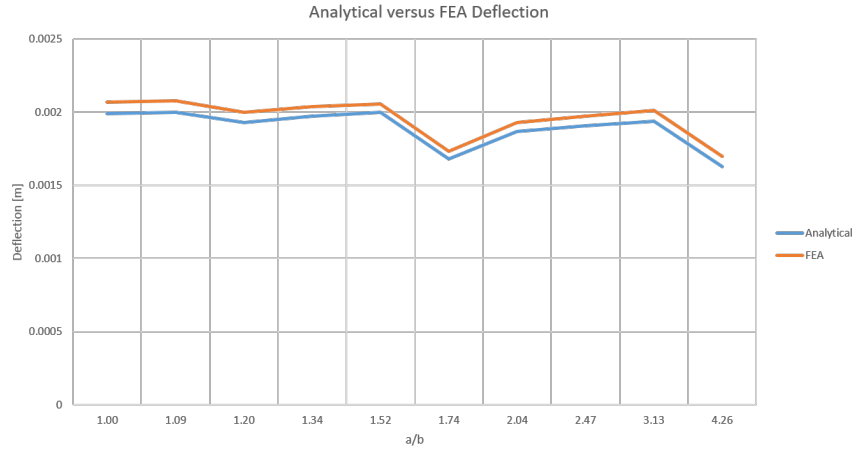

Figure 12. Panel pressure deflection

The last comparison checks whether the Tsai-Wu failure criterion as computed by the deterministic approach matches the one computed by the FEA. This way, the analytically predicted internal stresses are implicitly compared to those predicted by the FEA. Several panel size and load cases are run and the results are shown in Table 4. The Tsai-Wu failure values are checked at each ply and the highest values in the laminate are presented. From Table 4 it is clear that the analytical calculation under-predicts material failure. This means that a non-conservative design is obtained. However, to put this error into perspective, take the third panel from Table 4. When a 0 ply is added (in symmetry, so 2 plies in total), the FEA shows a Tsai-Wu failure value of 0.3054, which is slightly above the value obtained with the deterministic approach for the original panel. Considering an A320 fuselage, with 335 m^2 skin area, this results in a mass penalty of 164 kg, or 1.84 % of the total fuselage mass.

Table 4. Comparison of Tsai-Wu failure criterion between the analytical methods and the FEA. Note: $\bar{0}$ indicates a midply.

a	b	N_x	N_y	Layup	Analytical	FEA	Difference
[m]	[m]	[kN/m]	[kN/m]		Tsai-Wu [-]	Tsai-Wu [-]	[%]
0.5	0.3	250	500	$[\pm45/90_5/0/90_2/\pm45/\bar{0}]_s$	0.37	0.44	-17
0.5	0.5	500	500	$[\pm45/90_5/0/90_5/\pm45/90_3/0/90/\pm45/\bar{0}]_s$	0.50	0.56	-10
0.5	0.3	100	100	$[\pm45/90/0]_s$	0.29	0.36	-20
0.3	0.3	200	200	$[\pm45/90/0]_s$	0.66	0.72	-8.8
0.3	0.3	200	0	$[0]_s$	0.55	0.76	-29
0.3	0.3	0	200	$[90]_s$	0.55	0.76	-29
0.3	0.3	200	200	$[(\pm45)_2]_s$	0.66	0.72	-8.8

V. Case Study: Metal vs. Composite Fuselage

A study is performed to demonstrate the workings of the structural sizing methodology presented above and the associated mass estimation. A single-aisle aircraft is specified with similar top-level requirements as an A320-200 single-aisle medium range aircraft. Both a metal fuselage (Aluminum 7075) and an all-composite fuselage (material properties as in Table 3) are conceived assuming the same MTOM, MZFM, and payload mass.

American Institute of Aeronautics and Astronautics

In Figure 13 the smeared thickness of the outer skin panels, the frames and the stringers is shown in the sideview of the aircraft. The smeared thickness of a stringer or frame is defined as the cross-sectional area of the stringer or frame per unit skin area. Observing Figure 13(a), it may be concluded that sizing of the metal structure was done as expected. In the area where the wing load is introduced and largest compression is found in the keel quadrant of the fuselage, the stringer pitch is small and the smeared stringer thickness is high. In addition, the local skin panels are thicker there and the thickest frames are observed there as well. At the same position, but in the upper portion of the fuselage, a larger stringer smeared thickness is found, which is necessary to cope with the high tensile loads. Finally, the smallest stringers are observed in the side arc, where direct stresses are smallest (closest to the neutral axis).
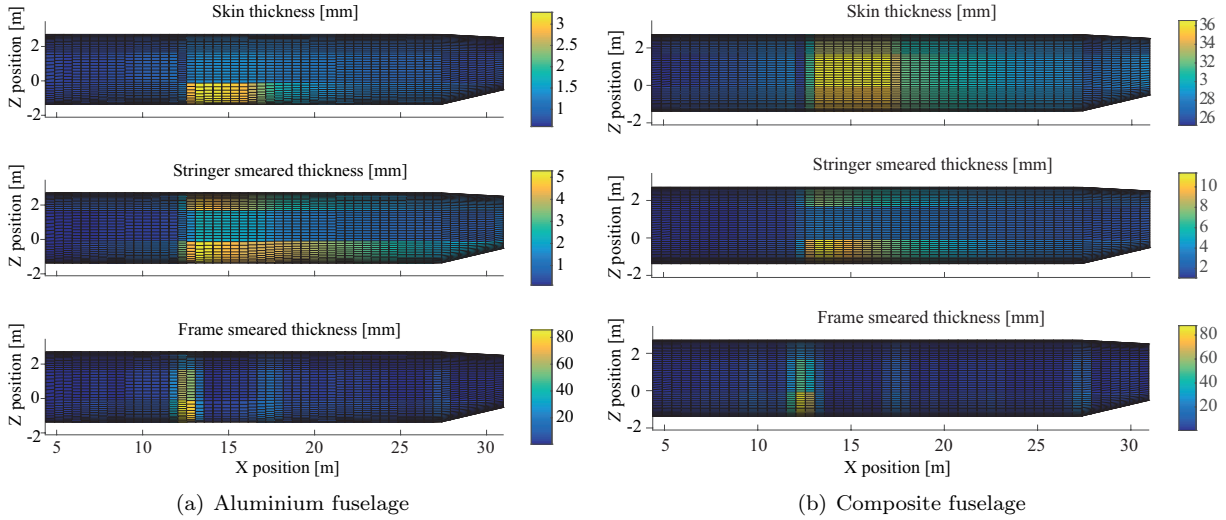

(a) Aluminium fuselage   (b) Composite fuselage

Figure 13. Airbus A320-200 thickness distribution

Also for the composite structure, sizing was done satisfactorily in the sense that the thickness distributions in Figure 13(b) are logical. Stringer pitch is small around the wing root, and stringer smeared thickness is increases there. The skin panels are thickest in the side arcs, where largest shear flows are present. Here, the direct stresses are smallest and, as a result, small stringer smeared thickness is observed. Finally, frames are sized similarly to the metal sizing and no oddities are seen there. Obviously, the thick frame at the wing root is a result from the wing loads being introduced at only that point.

The structural mass breakdowns of the aluminum and composite single-aisle aircraft are shown in Figure 14. The mass breakdowns for the composite A320-200 is shown in Figure 14(b). Immediately, it is observed that skins and stringers form most of the fuselage mass; around 50 %. The same trend was seen in Poland *et al.*[12] and Flynn *et al.*[13] The splicing and assembly portion is somewhat accounted for, albeit on the low end. Frames seem to form an acceptable portion of the fuselage mass.

VI.   Conclusion

A semi-analytical mass estimation method for pressurized, composite, oval fuselages has been developed. Pressurization loads in an oval fuselage section were compared to FEA results, and good agreement was obtained with errors less than one percent. Additionally, the implemented boom method showed good agreement with stresses predicted by FEA. It is therefore concluded that this method is implemented correctly and is able to satisfactorily predict internal stresses and shear flows. Computation of critical loads was compared to critical loads obtained from FEA. Shear buckling failure was found to be under-predicted by the implemented approach (i.e. the critical buckling load was overestimated) for panels with aspect ratio below 0.5. Scaling was used to compensate for this. For higher aspect ratios (up to 1), the opposite was found: a conservative shear buckling load was predicted. Deflection due to transverse pressure was compared with FEA and showed good agreement. Material failure due to tensile loads as predicted by the Tsai-Wu failure criterion seems to under-predict stresses as compared to FEA. Therefore, a non-conservative result is obtained. The method has been successfully applied to the design of a metallic and composite fuselage of a
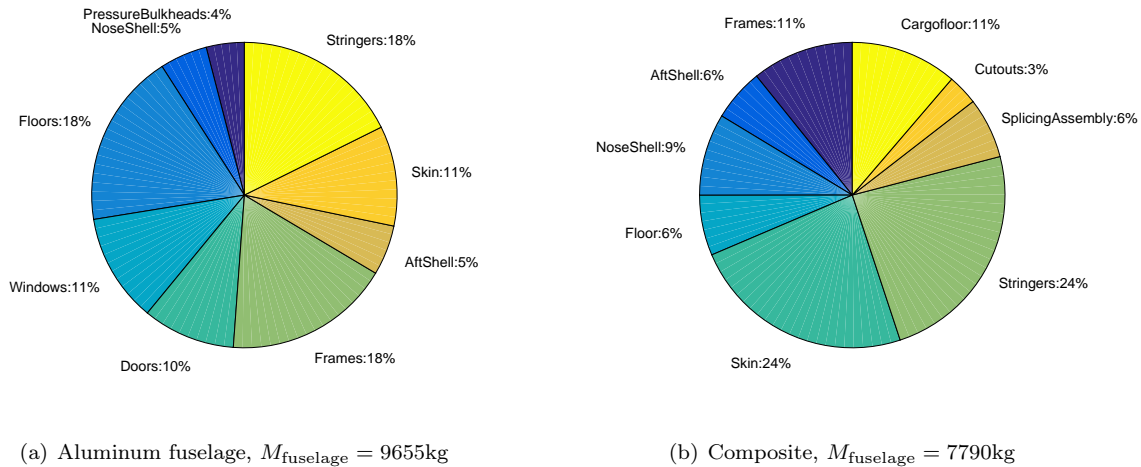
American Institute of Aeronautics and Astronautics

(a) Aluminum fuselage, $M_{\text{fuselage}} = 9655\text{kg}$

(b) Composite, $M_{\text{fuselage}} = 7790\text{kg}$

Figure 14. Mass breakdown of a single-aisle medium range aircraft similar to the Airbus A320.

single-aisle aircraft.

Acknowledgments

References

[1]Liebeck, R. H., "Design of the Blended Wing Body Subsonic Transport," *Journal of Aircraft*, Vol. 41, No. 1, 2004, pp. 10–25,
doi:10.2514/1.9084.

[2]J. M. M. Geuskens, F. J., Bergsma, O. K., Koussios, S., and Beukers, A., "Analysis of Conformable Pressure Vessels: Introducing the Multi-Bubble," *AIAA Journal*, Vol. 49, No. 8, 2011, pp. 1683–1692,
doi:10.2514/1.J050822.

[3]Mukhopadhyay, V., "Blended-Wing-Body Fuselage Structural Design for Weight Reduction," in "46th Structures, Structural Dynamics and Materials Conference," AIAA, April, 2005, pp. 1–8.

[4]Vos, R., Geuskens, F., and Hoogreef, M., "A New Structural Design Concept for Blended Wing Body Cabins," in "53rd AIAA/ASME/ASCE/AHS/ASC Structures, Structural Dynamics and Materials Conference," American Institute of Aeronautics and Astronautics, Honolulu, HW, 2012,
doi:doi:10.2514/6.2012-1998.

[5]Schmidt, K. and Vos, R., "A Semi-Analytical Weight Estimation Method for Oval Fuselages in Conventional and Novel Aircraft," in "52nd Aerospace Sciences Meeting," AIAA, January, 2014, pp. 1–20,
doi:doi:10.2514/6.2014-0026.

[6]Vos, R. and Hoogreef, M., "Semi-Analytical Weight Estimation Method for Fuselages with Oval Cross-Section," in "54th AIAA/ASME/ASCE/AHS/ASC Structures, Structural Dynamics, and Materials Conference," AIAA, 2013, pp. 1–15,
doi:10.2514/6.2013-1719.

[7]Howe, D., "Blended wing body airframe mass prediction," *Journal of Aerospace Engineering*, Vol. 215, No. June, 2001, pp. 319–331,
doi:10.1243/0954410011533329.

[8]Torenbeek, E., *Synthesis of Subsonic Airplane Design*, Delft University Press, Delft, 1982.

[9]de Smedt, S. and Vos, R., "Knowledge-Based Engineering Approach to the Finite Element Analysis of the Oval Fuselage Concept," in "53rd AIAA Aerospace Sciences Meeting," AIAA, January, 2015, pp. 1–15.

[10]Elmendorp, R. J. M., Vos, R., and LaRocca, G., "A Conceptual Design and Analysis Method for Conventional and Unconventional Aircraft," in Grant, I., ed., "Proceedings of the 29th Congress of the International Council for the Aeronautical Sciences," ICAS, St. Petersburg, Russia, 2014.

[11]Megson, T., *Aircraft Structures*, Elsevier, 4th ed., 2007.

[12]Polland, D., Finn, S., Griess, K., Hafenrichter, J., Hanson, C., Ilcewicz, L., Metschan, S., Scholz, D., and Smith, P., "Global Cost and Weight Evaluation of Fuselage Side Panel Design Concepts," Tech. rep., NASA, 1997.

[13]Flynn, B., Morris, M., Metschan, S., Swanson, G., Smith, P., Griess, K., Schramm, M., and Humphrey, R., "Global Cost and Weight Evaluation of Fuselage Keel Design Concepts," Tech. rep., Boeing Commercial Airplane Group, 1997.

[14]van Gent, I. and Kassapoglou, C., "Cost-weight trades for modular composite structures," *Structural and Multidisciplinary Optimization,*
doi:10.1007/s00158-013-1019-1.

[15]Jones, R., *Mechanics of Composite Materials*, Taylor and Francis, 2nd ed., 1999.

[16]Kassapoglou, C., *Design and Analysis of Composite Structures: With Applications to Aerospace Structures*, Wiley, 2nd ed., 2013.

[17]Bruhn, E., *Analysis and Design of Flight Vehicle Structures*, Tri-State Offset Company, 1973.

American Institute of Aeronautics and Astronautics